Short communication

Effect of vanadium redox species on photoelectrochemical behavior of TiO_2 and TiO_2/WO_3 photo-electrodes

Dong Liu [a], Fuqiang Liu [a,*], Jianguo Liu [b]

[a] Electrochemical Energy Lab, Department of Material Science and Engineering, University of Texas at Arlington, Arlington, TX 76019, USA
[b] Eco-materials and Renewable Energy Research Center, Department of Materials Science and Engineering, Nanjing University, Nanjing 210093, China

ABSTRACT

The photoresponse of bare TiO_2 and TiO_2/WO_3 hybrid electrodes was studied in a photoelectrochemical cell with VO^{2+} in 3 M sulfuric acid as the electrolyte. Linear sweep voltammetry study on both electrodes under AM1.5 illumination revealed a significant photoresponse enhancement compared to photolysis of water. This is attributed to the hole scavenging process initiated by quick redox reaction and depressed charge recombination at semiconductor/liquid interface. The photocurrent was boosted remarkably by factors of 57 and 78 on the bare TiO_2 and TiO_2/WO_3 hybrid electrode, respectively, when the VO^{2+} concentration increases from 0 to 1 M. This finding might render this approach a very promising way of solar energy conversion and storage. Photocharge/discharge process was also discovered on the WO_3 surface under different energy level of irradiation, leading to a deteriorated photocurrent.

Published by Elsevier B.V.

1. Introduction

The demand of energy has never been fulfilled for thousands of years and even exacerbated since the oil crisis in 1973. Alternative and sustainable energy sources such as solar, wind, tidal power, geothermal, hydroelectricity, bioenergy *etc.* are brought onto research and application agenda quickly as traditional coal and oil reserves are getting depleted. Among them, solar energy is considered to be the most reliable and inexhaustible source due to enormous energy supply of the sun [1].

In terms of solar energy conversion, apart from the well-established solid state junction systems often made of silicon, another very promising candidate system, photoelectrochemical cell (PEC), has been under extensive studies and development in past three decades despite its invention from photography since 1883 [1–7]. Numerous photoelectrochemical systems were proposed but most of them failed either with unacceptable energy conversion efficiency, poor chemical stability, or unreliable sustainability. The discovery by Fujishima and Honda in 1971 offered the prospect of using sunlight to produce environment-friendly fuel. However, the critical hurdle preventing its wide-

spread implementation is hydrogen handling. Although molecular hydrogen has very high energy density on a mass basis, as a gas at ambient conditions it has very low energy density by volume. Moreover, sluggish kinetics of photolysis of water and gas evolution reactions require a large electrochemical overpotential, which contributes to a low efficiency.

TiO_2 has been a favored photoelectrode material for such system due to its desirable intrinsic physical, chemical and commercial merits. Like everything balanced in nature, it also has its own imperfections—most representative of a wide bandgap which only allows absorption of ultraviolet region of the solar spectrum. In addition, the severe charge recombination at the semiconductor/liquid interface also hinders its further employment in solar energy conversion. Most of the effort devoted to ameliorate these issues has been unsatisfactory so far [7].

In this study, we demonstrate a novel approach to enhance the photoelectrochemical activity of semiconductor materials of TiO_2/WO_3 by using a vanadium redox (VO^{2+}) species. The goal is to explore regenerative solar energy storage using photocatalytic redox reaction, a new mode of solar energy storage with capability of harvesting significant portion of the visible spectrum. Our initial results demonstrate remarkable photoresponse of the redox component even with pristine TiO_2 as the photoanode catalyst. The inspiring results pose a very promising and alternative way of solar energy conversion and storage.

* Corresponding author. Tel.: +1 817 272 2704; fax: +1 814 272 2538.
E-mail address: fuqiang@uta.edu (F. Liu).

2. Experiment

2.1. Electrode preparation

Two types of photoeletrodes, TiO_2 and TiO_2/WO_3 were fabricated and used throughout the experiment with details elaborated elsewhere [8]. Anatase TiO_2 (99.7%, Alfa Aesar USA), ethyl cellulose (48.0–49.5%, Sigma-Aldrich USA), α-terpineol (laboratory grade, Fisher Scientific USA) were mixed in certain ratios under constant stirring at 80 °C for 1 h to obtain a uniform bare TiO_2 or hybrid paste with the addition of tungstic acid (Alfa Aesar USA) and hydrogen peroxide (35%, Alfa Aesar USA). All chemicals were used as received. Then the paste was deposited on a pre-cut square fluorine doped tin oxide (FTO) (sheet resistance 6–8 Ω/□, Pilkington USA) by using a doctor blade after mixing. The FTO substrate was pre-treated with acetone (99.7%, Fisher Scientific USA), methanol (99.8%, Fisher Scientific USA), deionized (DI) water (Millipore Simplicity@ USA), blow-dried and followed by heating in an oven at 120 °C for 1 h before the deposition. After the deposition, the obtained coating was dried in the oven for hours and then calcined with air flow at 325 °C for 5 min, 375 °C for 5 min, 450 °C for 15 min, and finally 500 °C for 15 min. The active area of the electrode is approximately 1 inch × 1 inch.

2.2. Electrolyte preparation

Stoichiometric amount of vanadium (IV) sulfate oxide hydrate ($VOSO_4 \cdot {}_xH_2O$) (99.9%, Alfa Aesar USA) was fully dissolved in 3 M sulfuric acid (96.6%, J.T. Baker USA) to form various molarity of $V–H_2SO_4$ electrolytes. These electrolytes are denoted as n M V–3 M H_2SO_4 for convenience of description in this study with nM and V representative of molar concentration and the vanadium redox species, respectively. The number of hydrate in $VOSO_4 \cdot {}_xH_2O$ was pre-determined by thermogravimetric analysis.

2.3. Characterization

The crystallographic information of the electrode material was determined by XRD (Siemens, 810-M340-32-C3000) at a scan rate $0.01° s^{-1}$ between 10° and 90° with a dwell time of 2 s. Photo-response of the PEC was determined by linear sweep voltammetry using an Advanced Electrochemical System (Princeton Applied Research, Parstat 2273) in a customized microbial cell where the photo-electrodes, i.e., TiO_2 and TiO_2/WO_3 coated on FTO, were attached as the working electrodes. Platinum mesh and Ag/AgCl electrode were used as counter and reference electrodes, respectively. Platinum wire and graphite sheet were also attempted as the working electrodes in comparison with the other two semiconductor electrodes during the experiment. The scan range of linear sweep voltammetry was from −0.197 to 1.3 V and the scan rate was set to 5 mV s^{-1}. The solar irradiation was created through an ozone-free solar simulator system (Newport USA) by using an AM1.5 global filter (81904, Newport USA) and other filters with different cut-on wavelength denoted as numbers in nm. For example, AM1.5+360 denotes AM1.5 spectrum with a cut-on wavelength at 360 nm. The standard AM1.5 irradiation was calibrated by a GaAs reference cell throughout the experiment.

3. Results and discussion

The linear sweep voltammograms of the bare TiO_2 electrode in various electrochemical conditions are compared in Fig. 1. 3 M sulfuric acid was chosen as the most suitable supporting electrolyte in terms of both stability and conductivity according to the study of Skyllas-Kazacos et al. [9]. Little difference in photoelectrochemical
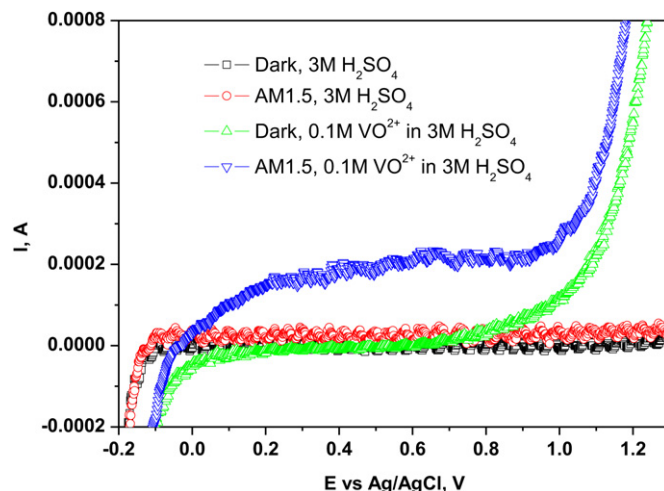

Fig. 1. The linear sweep voltammograms of the TiO_2 electrode in various electrochemical conditions.

response of the TiO_2 photoelectrode was observed regardless of the presence of illumination when only acid was employed as the electrolyte. Furthermore, the barely noticeable photocurrent throughout the potential window under illumination manifests the well-known wide bandgap of TiO_2 [10] and its notorious electron-hole pair recombination at the semiconductor/liquid junction interface. However, the addition of VO^{2+} species in the electrolyte abruptly changes the voltammetry response as seen in Fig. 1, especially under illumination. Not only can oxidation of the VO^{2+} species be seen at approximately 0.8 V (vs. Ag/AgCl, as the onset potential of oxidation) under both dark and illumination, but also the photocurrent of VO^{2+} oxidation is on average 14 times higher than that with only 3 M H_2SO_4 as the electrolyte throughout the entire potential window. The significant improvement in photo-response is believed to be induced by a synergistic effect of photocatalysis of TiO_2 and oxidation of VO^{2+} species. Fast electrochemical kinetics of VO^{2+} oxidation (at least six orders of magnitude higher than the oxygen evolution) is believed to quickly scavenge holes and increase the lifetime of electrons. This thus minimizes charge recombination and improves photocatalytic electron-transfer efficiency at the semiconductor interface [3].

In classic photoelectrochemistry of semiconductors [1–7,11], when light illuminates upon a n-type semiconductor immersed in a liquid solution containing a redox species, oxidative electron-transfer reaction occurs at the semiconductor interface once the electrolyte redox potential is positioned below that of the photo-generated hole at the edge of bended valence band of the semiconductor. As a result, the redox species will be oxidized photo-electrochemically. In our study, as the potential scale for the upper edge of valence band of TiO_2 against NHE (Normal Hydrogen Electrode) in contact with aqueous solution at pH 1 is approximately 2.8 V [7] and the standard potential of V^{4+}/V^{5+} redox is 1 V [12], it is obviously facile for the VO^{2+} species to be quickly oxidized by scavenging the holes at the semiconductor surface according to the principle mentioned above, which consequently reduces the electron-hole pair recombination and enhances the photoresponse. Note that the instability of voltammetry signals between 0.2 V and 0.8 V is believed to be caused by the possible competing scavenging process of photogenerated holes among a series of vanadium species complex [13–15] though V(IV) species exists predominantly in the form of VO^{2+} in pH <1 acidic solution [16].

Fig. 2 compares linear sweep voltammograms of four different electrodes in 0.1 M V–3 M H_2SO_4 electrolyte in the absence of
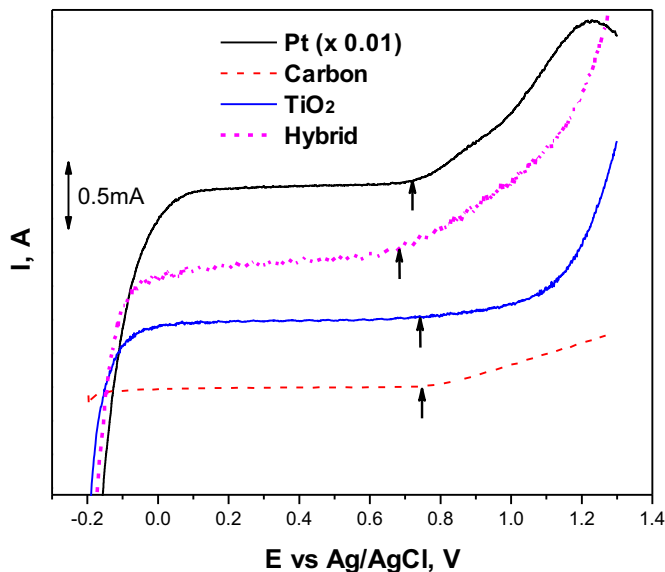
Fig. 2. Comparison of linear sweep voltammograms of 4 different electrodes in 0.1 MV−3 M H$_2$SO$_4$ electrolyte without illumination. The current of the Pt electrode has been divided by a factor of 100. The hybrid electrode contains 6 wt% of WO$_3$.

illumination. Their electrochemical behavior appears differently in geometry of the curve and the magnitude of the current. The anodic current due to oxygen evolution occurring at 1.23 V can be safely ruled out as illustrated in Fig. 1. The same electrochemical characteristics of the four electrodes, *i.e.,* curve shape and onset of

oxidation potential, confirm both electro- and photo-electrochemical oxidation of VO^{2+} observed in Fig. 1. The relative comparison of the electrochemical current indicates electrode activity. Carbon electrode is inactive toward vanadium oxidation. On the contrary, Pt electrode produces prominently larger current than all other electrodes. The TiO$_2$/WO$_3$ hybrid electrode results in a current increase at least by a factor of 2 than that produced by the bare TiO$_2$ electrode. This enhanced catalytic property in the employed electrolyte system is probably due to a relative faster charge transfer process at the surface of the hybrid electrode. In the figure, the negative shift of onset potential of VO^{2+} oxidation (labeled by an arrow) for the TiO$_2$/WO$_3$ hybrid electrode further confirms the enhancement in charge transfer in the hybrid electrode (similar to electron conductors as Pt and carbon) than that for bare TiO$_2$.

The effect of vanadium species concentration on linear sweep voltammogram of both the bare TiO$_2$ and TiO$_2$/WO$_3$ hybrid electrodes under dark and illumination is presented in Fig. 3 and Table 1. The curves in Fig. 3(b)–(d) are very similar in shape but differ apparently from that in Fig. 3(a) due to oxidation of vanadium species. The current produced on the hybrid electrode becomes progressively negative with the decrease of the applied potential in the graphs, which is ascribed to the photocharge process occurred in the WO$_3$ [19–21]. Note that the weak and flat peak that appears around −0.1 V in Fig. 3(a) for the hybrid electrode when vanadium species is not involved in the electrolyte is unassured and suspected to be the redox transition of W^{5+}/W^{6+} [22] regardless of illumination. On the other hand, the current boost on both bare TiO$_2$ and TiO$_2$/WO$_3$ hybrid electrode with the addition of vanadium species illustrated in both Fig. 3 and Table 1 is indisputable, especially in the presence of illumination.
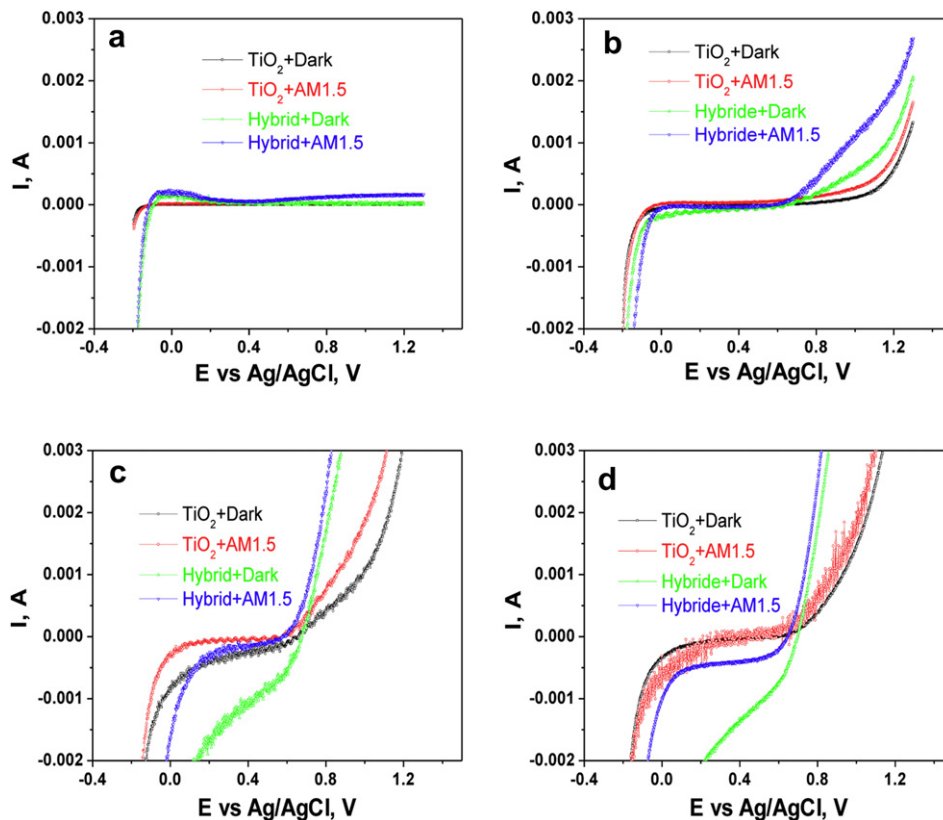

Fig. 3. The effect of VO^{2+} concentration on photoresponse of the bare TiO$_2$ and TiO$_2$/WO$_3$ (6 wt% WO$_3$) hybrid electrodes under dark and illumination: (a) 0 M, (b) 0.1 M, (c) 0.5 M, and (d) 1 M.

Table 1
The numerical presentation of effect of vanadium species concentration on linear sweep voltammogram of bare TiO_2 and TiO_2/WO_3 (6 wt% WO_3) hybrid electrodes under dark and illumination. The acronyms are: T-TiO_2; D-dark; H-hybrid; A-illumination at AM1.5.

VO^{2+} conc (M)	Current @ 1.0 V (μA)			
	T + D	T + A	H + D	H + A
0	0.93	21.32	7.3	153.15
0.1	110.31	263.73	532.65	1110.00
0.5	1070.00	1910.00	5320.00	7290.00
1	1470.00	1660.00	6690.00	8780.00

The above results can be explained by the relative position of band edges of TiO_2 and WO_3, which is illustrated in many literatures [17–20]. Electrons excited to the TiO_2 conduction band under illumination tend to go "downhill" into the conduction band of WO_3 due to more positive potential of the latter, and holes if generated from WO_3 go "uphill" to the valence band of TiO_2 and are trapped at the surface. These holes will easily oxidize VO^{2+} species in the electrolyte at the semiconductor/liquid interface and cause a current increase. Furthermore, this also reduces the probability of electron–hole pair recombination at the interface. With the increase of vanadium species concentration from 0 to 1 M in the electrolyte, the photocurrent at potential of 1.0 V increases remarkably by a factor up to 57 and 78 on the bare TiO_2 and TiO_2/WO_3 hybrid electrodes, respectively, as seen in Table 1, which explicitly results from the effective hole scavenging process by the VO^{2+} species explained earlier. Apparent flat band potential of the hybrid electrode was also observed to shift negatively compared to the bare TiO_2 electrode, indicating improved charge separation. Note that the apparent flat band potential is defined as zero-current potential of semiconductor materials under illumination [23].

An interesting phenomenon was observed on the photoresponse of the hybrid electrode shown in Fig. 4. The photocurrent is not scaled up to the energy level of irradiation but instead decreases as seen in the graph. We ascribe this occurrence to the formation of tungsten bronze induced by the photocharge/discharge process under higher energy irradiation on the WO_3 surface. It is known that WO_3 tends to be electrochemically reduced to tungsten bronze by combining electrons and protons (H^+) under higher energy irradiation (In our case, under AM1.5 and AM1.5+360 irradiation) as depicted in the following equation [19–21]:

$$WO_3 + xe^- + xH^+ \underset{\text{discharge}}{\overset{\text{photocharge}}{\rightleftarrows}} H_xWO_3$$
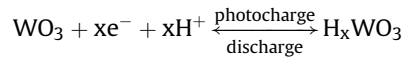
Due to such reaction, the surface of the photocatalysts, *i.e.*, TiO_2 and WO_3, will be covered with H_xWO_3, which prevents the photogenerated holes from moving from the valence band of WO_3 to that of TiO_2 and further to semiconductor/liquid interface to oxidize VO^{2+} species. This thus compromises photocatalysis of the semiconductor materials. When irradiation shifts to lower energy level (In our case, under AM1.5+455 and AM1.5+515), tungsten bronze undergoes rapid discharge/self-discharge, which transforms itself back to WO_3. As a result, more semiconductor material will rejoin the photocatalysis process. Furthermore, the transfer of the photogenerated holes may be again possible from the WO_3 valence band to the TiO_2 valence band, thus enhancing the photocurrent. This photocharge/discharge process was confirmed by the blue appearance of the electrode under higher energy irradiation and disappearance under lower one. It is also found that the decrease of photocurrent incurred by this photocharge/discharge process is independent on vanadium species concentration.

The optical transition of various hybrid electrodes was studied by UV–vis diffuse reflectance spectroscopy with results revealed in Fig. 5. Note that the optical transition of the bare TiO_2 is not shown in the graph due to negligible difference compared to the hybrid electrodes. The absorption shoulder starts from the UV region at around 380 nm due to absorbance of TiO_2. The absorption edge undergoes a redshift with increasing load of WO_3 in the hybrid electrodes, extending the absorbance of light from the UV region to visible region due to lower bandgap energy of WO_3 compared to TiO_2. The intensity of absorption is also increased. Such improvement in absorption is in good agreement with the photocurrent boost as demonstrated in Fig. 3 and Table 1. It is also concluded that WO_3 is not incorporated into the TiO_2 crystal lattice [24–28] due to the overlap of the absorption shoulders on all four curves in Fig. 5. The crystallographic information of freshly-made bare TiO_2 and TiO_2/WO_3 hybrid electrodes is presented in Fig. 6. It clearly reveals individual diffraction peaks of each compound and the corresponding crystal structures are determined by cross-referencing JCDPS of the anatase TiO_2 (#21-1272) and polycrystalline WO_3 (#83-0950). No rutile or bromite phase of TiO_2 is found and the
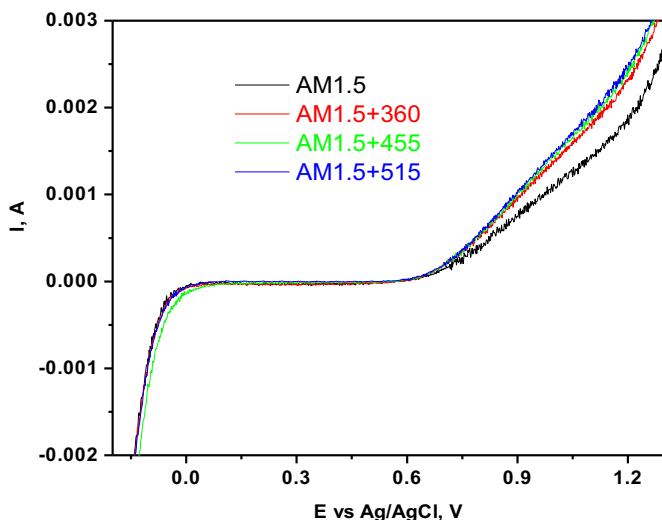

Fig. 4. The effect of illumination level on photoresponse of the hybrid electrode (6 wt% WO_3) in 0.1 M V–3 M H_2SO_4 electrolyte.
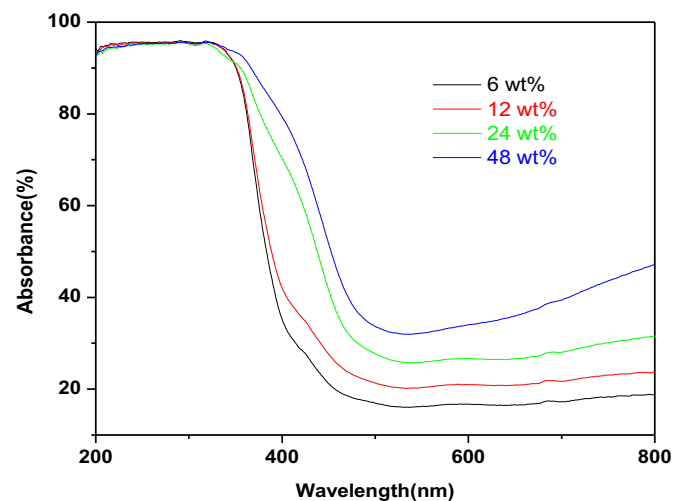

Fig. 5. UV–vis diffuse reflectance spectra of hybrid electrodes with different WO_3 weight fractions.
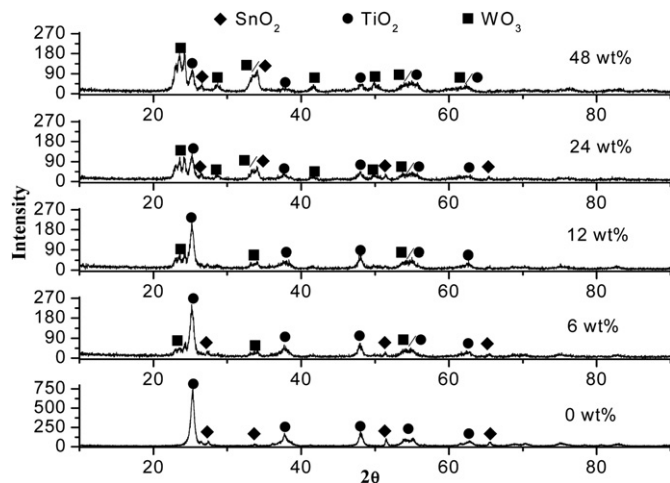
Fig. 6. XRD results of freshly-made bare TiO_2 and TiO_2/WO_3 hybrid electrodes.

WO_3 phase is primarily crystalline. The SnO_2 signal (#77-0452), shown in all the diffraction patterns obtained, is from the FTO substrate.

4. Conclusion

The bare TiO_2 and TiO_2/WO_3 hybrid electrodes were fabricated on FTO substrate and their photoelectrochemical properties were investigated. Linear sweep voltammetry tests show a pronounced photoresponse enhancement on both electrodes when vanadium species was added to the electrolyte, which is due to reduced electron-hole pair recombination by hole scavenging of the VO^{2+} species. The photocurrent was boosted remarkably by factors of 57 and 78 on the bare TiO_2 and TiO_2/WO_3 hybrid electrode, respectively, when the VO^{2+} concentration increases from 0 to 1 M. The UV–vis diffuse reflectance spectroscopy indicates a redshift of the absorption edge with the increase of WO_3 in the hybrid electrodes, confirming the photocatalytic enhancement of the hybrid electrode. A photocharge process that occurs on the WO_3 surface in the hybrid electrode at higher energy irradiation was found to form the tungsten bronze to decrease the photocurrent whereas a discharge process releases it back to WO_3 under lower energy irradiation.

References

[1] Allen J. Bard, Science 207 (1980) 139.
[2] Allen J. Bard, J. Photochem. 10 (1979) 59.
[3] Adam Heller, Acc. Chem. Res. 14 (1981) 154.
[4] Yu. V. Pleskov, Prog. Surf. Sci. 15 (1984) 401.
[5] R.N. Pandey, K.S. Chandra Babu, O.N. Srivastava, Prog. Surf. Sci. 52 (1996) 125.
[6] Nikola Getoff, Int. J. Hydrogen Energy 15 (1990) 407.
[7] Michael Grätzel, Nature 14 (2000) 338.
[8] D. Liu, F. Liu, 221st Electrochemical Society Meeting, Abstract 184, Seattle, Washington, May 6–10 (2012).
[9] M. Kazacos, M. Cheng, M. Skyllas-Kazacos, J. Appl. Electrochem. 20 (1990) 463.
[10] Akira Fujishima, Kenichi Honda, Nature 238 (1972) 37.
[11] Yu. V. Pleskov, Yu. Ya. Gurevich, Semiconductor Photoelectrochemistry, (1986).
[12] Allen J. Bard, Roger Parsons, Joseph Jordan, Standard Potentials in Aqueous Solution, Chap. 17, 520, (1985).
[13] M. Gattrell, J. Park, B. MacDougall, J. Apte, S. McCarthy, C.W. Wu, J. Electrochem. Soc. 151 (2004) A123.
[14] Gaku Oriji, Yasushi Katayama, Takashi Miura, Electrochim. Acta. 49 (2004) 3091.
[15] Gaku Oriji, Yasushi Katayama, Takashi Miura, J. Power Sources 139 (2005) 321.
[16] J.O. Hill, I.G. Worsley, L.G. Hepler, Chem. Rev. 71 (1971) 729.
[17] Irina Shiyanovskaya, Maria Hepel, J. Electrochem. Soc. 145 (1998) 3981.
[18] Irina Shiyanovskaya, Maria Hepel, J. Electrochem. Soc. 146 (1999) 243.
[19] Shinya Higashimoto, Nobuya Kitahata, Kohichi Mori, Masashi Azuma, Catal Lett. 101 (2005) 49.
[20] Shinya Higashimoto, Yoshiaki Ushiroda, Masashi Azuma, Top Catal. 47 (2008) 148.
[21] Tetsu Tatsuma, Shuichi Saitoh, Yoshihisa Ohko, Akira Fujishima, Chem. Mater. 13 (2001) 2838.
[22] V. Raghuveer, B. Viswanathan, J. Power Sources 144 (2005) 1.
[23] Vaidyanathan Subramanian, Eduardo Wolf, Prashant V. Kamat, J. Phys. Chem. B 105 (2001) 11439.
[24] Chen Shifu, Chen Lei, Gao Shen, Cao Gengyu, Powder Technol 160 (2005) 198.
[25] V. Iliev, D. Tomova, S. Rakovsky, A. Eliyas, G. Li Puma, J. Mol Catal. A-Chem. 327 (2010) 51.
[26] J. He, Q.Z. Cai, D. Zhu, Q. Luo, D.Q. Zhang, X.W. Li, X. Zhao, W. Sun, Curr. Appl. Phys. 11 (2011) 98.
[27] M.R. Bayati, F. Golestani-Fard, A.Z. Moshfegh, R. Molaei, Mater. Chem. Phys. 128 (2011) 427.
[28] Kezhen Lv, Jie Li, Xiaoxia Qing, Wenzhang Li, Qiyuan Chen, J. Hazard Mater. 189 (2011) 329.